Performance of a Counterflow Virtual Impactor in the NASA Icing Research Tunnel

C. H. TWOHY

National Center for Atmospheric Research, Boulder, Colorado

J. W. STRAPP

Meteorological Service of Canada, Toronto, Ontario, Canada

M. WENDISCH

Institute for Tropospheric Research, Leipzig, Germany

(Manuscript received 14 February 2001, in final form 18 September 2002)

ABSTRACT

A counterflow virtual impactor (CVI) designed for aircraft use was evaluated at the NASA Icing Research Tunnel in Cleveland, Ohio. Tests were conducted for tunnel speeds of 67 and 100 m s^{-1}, for liquid water contents of 0.23–1.4 g m^{-3}, and for a wide range of droplet median volume diameters (MVDs). For droplet distributions with MVDs between about 30 and 240 μm, liquid water content (LWC) measured by the CVI agreed with reference values within the uncertainty of the measurements. For a range of LWCs at 30-μm MVD, the relationship was near 1:1, and no systematic dependence of CVI results on LWC or airspeed was observed. For smaller MVDs, the CVI underestimated LWC. Decreased collection efficiency for small droplets can partially explain this effect, but the difference from reference values was larger than expected based on previous calibrations and comparisons with in situ data. Tunnel runs conducted with a flow-straightening shroud around the CVI inlet produced approximately 20% enhancements in LWC at small MVDs, which are expected for these speeds based on previous modeling studies. The effect of large drop breakup on CVI droplet number concentration was evaluated both theoretically and experimentally; drop breakup was predicted to occur for drops larger than 169 μm at 67 m s^{-1} and larger than 76 μm at 100 m s^{-1}. Enhancement in number concentration measured by the CVI was found to be strongly related to observed large drop concentrations, particularly to those in the 312–700-μm-diameter range.

1. Introduction

In September and October 1998, an assessment of cloud physics instrumentation was conducted at the Icing Research Tunnel (IRT) at the National Aeronautics and Space Administration (NASA) Glenn Research Center. The performance of a large number of cloud microphysical probes currently used for research was evaluated under a variety of conditions. Results from tunnel measurements using a counterflow virtual impactor (CVI) are presented here.

Tests were conducted for tunnel speeds of 67 and 100 m s^{-1}, for liquid water contents of 0.23–1.4 g m^{-3}, and for a wide range of droplet median volume diameters (MVDs). The IRT is large enough to test multiple instruments at once (about 2 m high by 3 m wide). It is calibrated and characterized in terms of liquid water content with accepted reference techniques (icing blade and rotating icing cylinder). An overview of the tests and instrument results is presented by Strapp et al. (2003, this issue), and a summary of the performance of the airborne Particle Volume Monitor (PVM) is given by Wendisch et al. (2002).

2. CVI description

The CVI (Ogren et al. 1985; Noone et al. 1988; Twohy et al. 1997) has been utilized both in the air and on the ground in studies of aerosol–cloud interactions, cloud physics, and climate. At the CVI inlet tip, cloud droplets or ice crystals larger than a certain aerodynamic diameter are separated from the interstitial aerosol and water vapor and impacted into warm, dry carrier gas. This separation is accomplished using a counterflow stream of gas that is supplied through a porous tube inside the CVI tip and that only larger (cloud) particles are able to penetrate (Fig. 1). Droplets or crystals are evaporated within the inlet at a temperature of about 50°C, and the water vapor and nonvolatile residual nuclei remaining after droplet evaporation are measured

Corresponding author address: C. H. Twohy, Oregon State University, Ocean Admin. 104, Corvallis, OR 97331.
E-mail: twohy@coas.oregonstate.edu

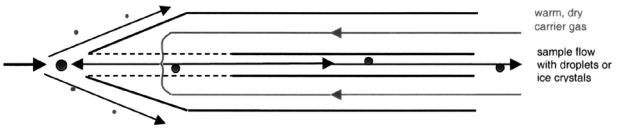

FIG. 1. Schematic of the CVI inlet probe tip. Warm, dry carrier gas (gray lines) is pumped to the tip and radially in through a porous tube, where it splits into the sample flow and the counterflow, which exits the probe tip. Larger droplets or ice crystals (depicted as large spheres) approaching the tip have sufficient inertia to penetrate the counterflow and enter the sample flow, while unactivated aerosol particles and small droplets (depicted as small spheres) follow the airflow streamlines around the probe tip.

downstream of the inlet with selected instruments. These may include a Lyman-alpha or similar hygrometer, a condensation nucleus counter, an optical particle counter, and particle filters for chemical analyses. Because droplets or crystals in a large sampling volume are impacted into a relatively small sample stream, their number concentrations and water contents within the CVI are significantly enhanced over their ambient values. This enhancement factor is equal to the ratio of the air sample flow rate impinging on the probe tip to the sample flow rate within the inlet probe. This enhancement and the rejection of ambient water vapor permit detection of ice water contents as low as 1 mg m^{-3} in cirrus clouds (e.g., Ström and Heintzenberg 1994). Ice water contents measured by the CVI and PVM in orographic wave clouds with predominantly small (<30 μm diameter) ice crystals showed excellent agreement (Gerber et al. 1998).

A CVI designed at the National Center for Atmospheric Research (NCAR) and flown on their Lockheed Electra aircraft was tested in the IRT. A standard Lyman-alpha hygrometer was used downstream of the inlet as the sensor for water content, and a TSI 3760 condensation nucleus counter was used to measure particle number concentration. For the Lyman-alpha, the baseline value (offset) obtained before the droplet spray was introduced into the tunnel was subtracted from the liquid water content (LWC) signal with the spray on. LWCs presented here are corrected for the enhancement factor within the CVI and are 60-s averages.

The impaction characteristics of the CVI are determined by inlet geometry, airspeed, and ambient conditions. Experimental calibrations of the size of unit-density particle that is sampled with 50% efficiency (''cut size'') have in the past agreed well with the CVI cut size that is calculated from theory (Noone et al. 1988). Calibrations by Anderson et al. (1993) and Schwarzenböck and Heintzenberg (2000) expanded upon the Noone et al. methods. Important CVI design parameters that affect cut size (and their corresponding values for this CVI probe inlet) include the outside tip radius (4.2 mm), the length of solid material (4.0 mm) ahead of the porous tube within the inlet, and the porous tube length (75 mm). Since the NCAR CVI tip shape is similar to that of the ''mini CVI'' designed by Anderson et al. (1993), cut sizes were calculated based on their results. Following that study, a scaling factor of 0.8 was used to account for the effect of the outside radius on cut size. For our geometry and the CVI operating conditions during the IRT tests (987 mb and 40°C), resulting cut sizes were 8.2- and 9.6-μm diameter, respectively, for airspeeds of 100 and 67 m s^{-1}. LWC data presented in this paper have not been adjusted for the reduced collection efficiency of droplets near the CVI cut size.

Ground-based CVIs with substantially smaller cut sizes have been designed by using higher impaction velocities and smaller inlet diameters (Anderson et al. 1993; Schwarzenböck and Heintzenberg 2000). However, impaction velocity is determined by the aircraft airspeed for airborne probes, and smaller inlet diameters also mean smaller sampling volumes, which may limit large drop collection and certain chemical analyses.

Uncertainty in the CVI liquid water content measurement is induced by flow and geometry considerations related to the enhancement factor within the CVI (estimated uncertainty of 8%), and by calibration, offset, and hysteresis factors related to the Lyman-alpha hygrometer (estimated at 5%, 10%, and 5%, respectively). Combination of the above uncertainties via accepted engineering methods (Coleman and Steele 1999) leads to an overall uncertainty (95% confidence level) in CVI LWC for these tests of about 15%.

3. CVI performance

a. Liquid water content as a function of droplet MVD

A series of 54 tunnel runs at various LWCs was made at a range of MVDs and two different airspeeds on 1 October 1998. The measured ratio of CVI LWC to the tunnel reference LWC as a function of MVD is presented in Fig. 2. Strapp et al. (2003) quote an overall 2σ uncertainty of approximately 12% for individual LWC values at MVDs less than or equal to about 30 μm, and 20% for larger MVDs. Vertical error bars for CVI/tunnel LWC ratios represent 19% or 25% uncertainty, depending on MVD (based on 15% uncertainty in the CVI LWC and 12% and 20% uncertainties in the tunnel LWC for MVDs ≤ 30 μm and >30 μm, respectively).

Many airborne instruments size droplets by optical means; those probes produced by Particle Measuring Systems, Inc. (PMS) include the Forward Scattering Spectrometer Probe (FSSP), and the 2D-C, 2D-P, 230-X, and 1D-P probes, discussed below. For Fig. 2 and elsewhere in this paper, MVDs have been calculated from the composite Phase Doppler Particle Analyzer (PDPA), 2D-C, and 2D-P distributions measured during these particular tests.[1] As discussed by Strapp et al.

[1] MVDs derived from the PDPA were not available for all the 100 m s^{-1} test points; in these cases, MVDs from 67 m s^{-1} for the same tunnel nozzle conditions were used. This is a recommended practice by the Society of Automotive Engineers for calibration and acceptance of icing wind tunnels (Strapp et al. 2003).

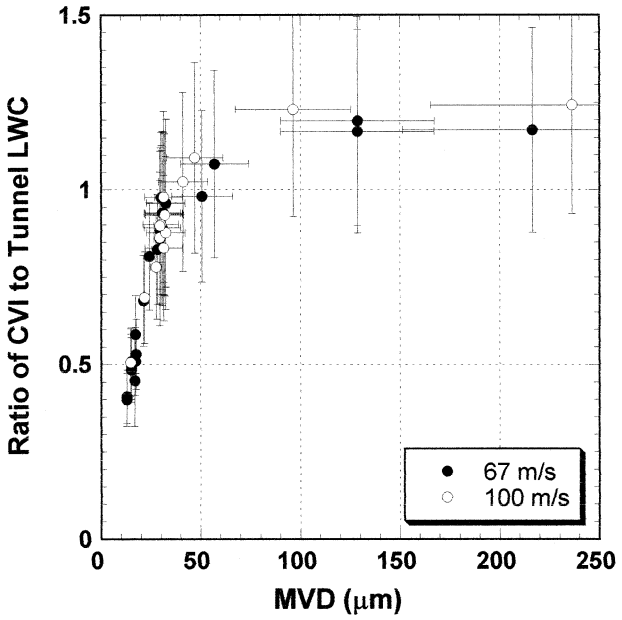

FIG. 2. Ratio of CVI LWC to tunnel LWC as a function of median volume diameter (derived from PDPA and 2D probe spectra) for two different airspeeds. Horizontal error bars on MVDs here and in other figures represent the estimated uncertainties of 10% and 30% for MVDs ≤ 30 μm and >30 μm, respectively; conditions near 30-μm MVD with larger uncertainty as discussed by Strapp et al. (2003) have not been included. Vertical error bars represent estimated uncertainties in the CVI to tunnel LWC ratio of 19% and 25% for MVDs ≤ 30 μm and >30 μm, respectively. The lowest MVD runs at 100 m s^{-1} have not been included for the reasons discussed by Strapp et al.

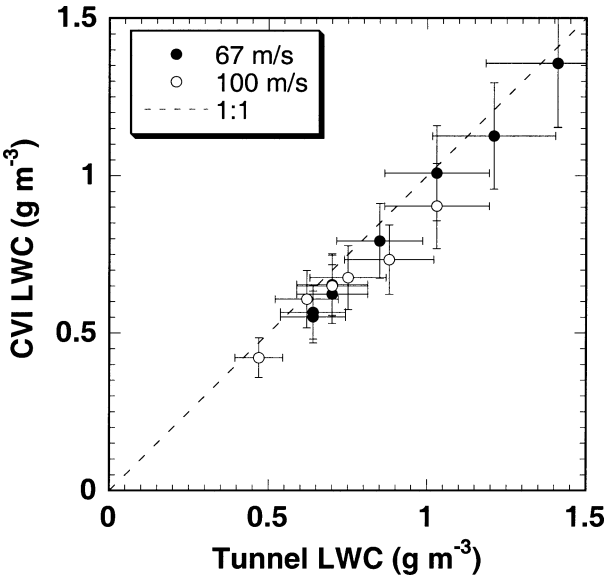

FIG. 3. CVI LWC vs tunnel LWC at median volume diameters of about 30 μm. Strapp et al. (2003) estimated uncertainty in tunnel LWC as 12% for MVDs ≤ 30 μm and 20% for MVDs >30 μm; since the actual MVDs used here range from 29.5 to 32.5 μm, horizontal error bars represent an average uncertainty of 16%. Vertical error bars reflect the CVI LWC uncertainty of about 15%.

(2003), the MVDs normally quoted by NASA are derived from earlier calibrations with a PMS FSSP, 230-X, and 1D-P, and are generally larger than those derived from the PDPA, 2D-C, and 2D-P. Large numbers of very small droplets are generated for small-MVD runs (for our tests, usually greater than 1000 cm^{-3}). For these conditions, FSSP sizing errors related to particle coincidence are large and undefined, potentially resulting in large errors in FSSP MVDs. MVDs derived from PDPA + 2D − C + 2D − P composite spectra, when integrated to obtain LWC, agree better with the tunnel LWC values and are not subject to large coincidence errors. Therefore, we follow Strapp et al. (2003) and utilize the PDPA-derived MVDs, or ''study'' MVDs. Strapp et al. estimates uncertainty in the study MVDs to be 10% for MVDs ≤ 30 μm at 67 m s^{-1} and as great as 30% for larger MVDs. Uncertainty in the smaller MVDs may be higher at 100 m s^{-1}, however, due to the larger uncertainties in the PDPA sample volume correction. For more information, see the detailed discussion by Strapp et al. (2003).

Figure 2 shows that within the uncertainty of the measurements, the ratio of CVI to tunnel LWC values is near 1.0 for MVDs ≥ 30 μm. For these conditions, the CVI and tunnel reference LWC agree within the expected 25% uncertainty for their ratio. The largest departures occur for MVDs of 100 μm and larger, at which the tunnel LWCs are the most uncertain. Response to a range of different LWCs was assessed for droplet distributions with MVDs of about 30 μm, at which CVI cut size effects should be negligible. Results are shown in Fig. 3. For all points, the CVI LWC matches the tunnel LWC within the measurement uncertainty, and no systematic dependence on LWC or airspeed is apparent.

For MVDs smaller than 30 μm, the CVI LWC is substantially lower than the tunnel LWC. This can be partially explained by the decreased collection efficiency of the CVI for small droplets, which do not fully penetrate the counterflow inside the CVI tip. Figure 4 shows the expected versus measured LWC ratios in the small-MVD size range, using two different collection efficiency curves that have been empirically determined for other versions of the CVI by Anderson et al. (1993) and Noone et al. (1988). The measured ratios are substantially lower than expected from either previous calibration in the 12–25 μm MVD range. Thus, either the CVI collection characteristics are different than determined by previous calibration, the small droplet size distributions in the tunnel are inaccurate, or both factors are important. This aspect of CVI performance, which is not well understood, is explored further in the appendix, which includes more details of CVI calibration techniques, as well as field data comparisons of the CVI with FSSP-100 number concentrations. These comparisons with the FSSP show better agreement with the expected CVI collection characteristics than observed in the IRT (Fig. 4).

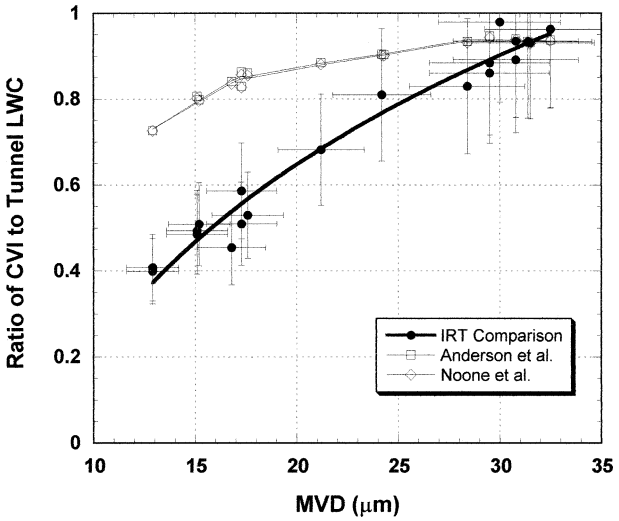

FIG. 4. Measured response function of the CVI for 67 m s^{-1} runs with MVDs up to about 30 μm vs expected response using two different collection efficiency curves (see text).

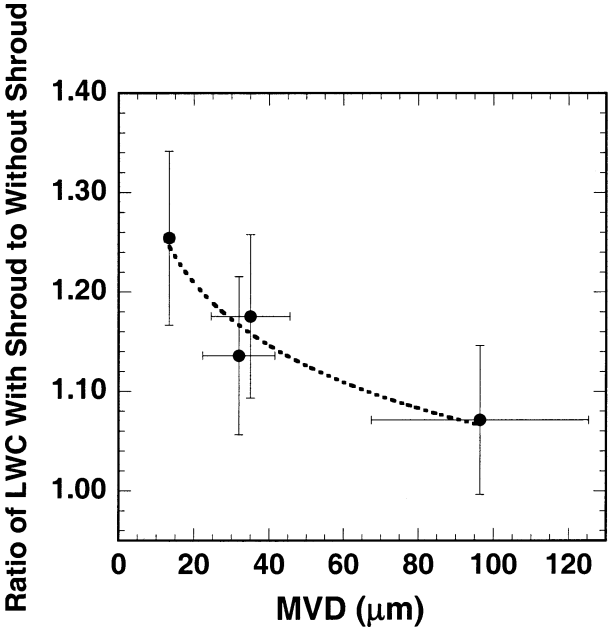

FIG. 5. Ratio of CVI LWC with and without the flow-straightening shroud, as a function of median volume diameter. Vertical error bars reflect an estimated uncertainty in the ratio of CVI LWC measurements of 7% (smaller than the uncertainty in the LWC itself due to fixed bias errors).

b. Effect of shroud

A few 100 m s^{-1} tunnel conditions were run with and without a flow-straightening shroud around the CVI inlet. When used on an aircraft, a shroud has the benefit of aligning the impinging airflow with the CVI inlet tip, thereby stabilizing the counterflow and minimizing the off-axial trajectories of droplets. The shroud was originally designed to be isokinetic on the NASA DC-8 aircraft at transonic airspeeds (approximately 225 m s^{-1} and Mach $>$ 0.8). At lower airspeeds, computational fluid dynamical (CFD) modeling predicts airflow within the shroud to be superisokinetic by about 20% (Twohy 1998). Small droplets should respond to these airspeed changes, thus increasing the effective sampling volume impinging on the CVI tip by about 20%. A comparison of CVI LWCs with and without the shroud as a function of MVD is shown in Fig. 5.

LWC values are, on average, about 19% higher with the shroud than without it for small droplet sizes, approximately as expected based on the CFD results. Thus, a 20% airspeed correction factor may be applied when sampling with the shroud at low airspeeds in clouds without large hydrometeors.

c. Number concentration and drop breakup

The CVI also can be used to measure droplet number concentration, since residual nuclei from droplets after evaporation are measured with a condensation nucleus counter. While droplets generated by spray bars in the IRT are not formed on a cloud condensation nucleus as in real clouds, small levels of impurities naturally present in the water will precipitate out upon droplet evaporation and have a similar effect. Residual particles as small as about 0.01 μm are counted by the TSI Model 3760 counter used.

The droplet sizes that can be counted in this way range from the lower cut size to the upper cut size, which is the size of (partially evaporated) droplets that will impact on the 90° bend downstream of the CVI inlet tip. Based on calculations of droplet motion and evaporation (Anderson and Twohy 1993), the upper cut size for the CVI used in the IRT is about 50-μm diameter. Number concentrations measured in this way are only accurate if one droplet produces one, and only one, residual nucleus. Calibrations and field studies have shown that this is usually the case for droplets between the minimum cut size and upper cut size, unless impaction speeds are high or very large hydrometeors are present. Under these conditions, drag stresses that drops will experience upon impaction can exceed the surface tension holding them together. Consequently, they may break up and produce multiple small droplets (Twohy 1992; Schwarzenböck and Heintzenberg 2000). These droplets will subsequently evaporate, and their water mass will be measured downstream by the hygrometer without adversely affecting the CVI measurement of LWC. However, the apparent CVI number concentration may be enhanced, since each small droplet will also contain solute that produces its own residual particle upon drop evaporation. The different drop distributions generated in the NASA tunnel provided a good opportunity to test which drops participate in the breakup phenomenon.

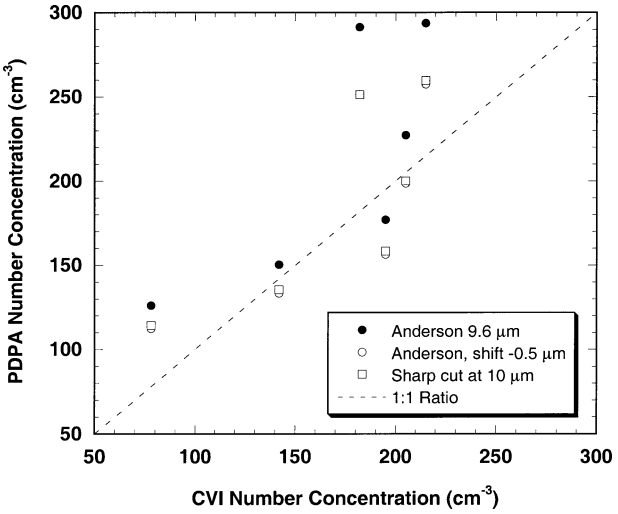

FIG. 6. Comparison of measured CVI number concentration with that calculated from the PDPA distribution in different ways, for small-MVD runs at 67 m s^{-1}. The solid circles use the Anderson et al. (1993) collection efficiency curve and the number concentrations based on the PDPA channel midpoint, the hollow circles use the PDPA channel midpoint minus 0.5 μm, and the hollow squares assume zero collection below 10.0 μm and 100% collection above 10.0 μm.

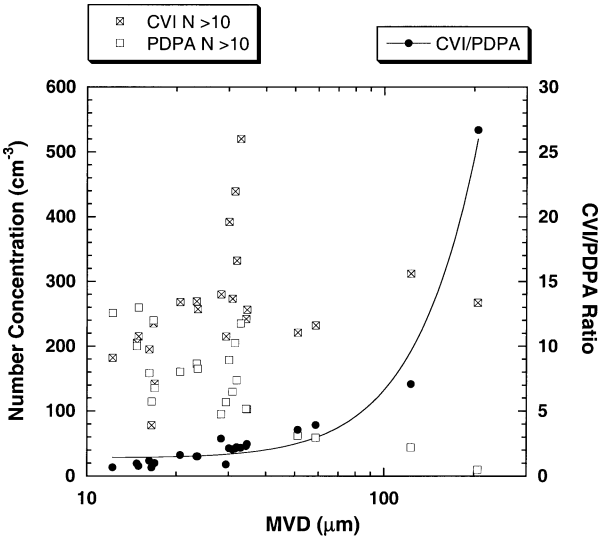

FIG. 7. CVI and PDPA number concentrations larger than 10.0 μm, and the ratio between the two, as a function of median volume diameter at 67 m s^{-1}.

CVI number concentrations were compared to number concentrations determined from the PDPA measurements for corresponding runs. The PDPA number concentrations were corrected by a single scale factor for each airspeed based on the slope of the linear relationship between tunnel LWC and PDPA LWC (e.g., Strapp et al. 2003). This scale factor was corroborated to some degree by the resulting relatively good agreement between FSSP and scaled-PDPA concentrations, except when FSSP concentrations were very high and that probe was suspected to be near saturation. Figure 6 compares the measured CVI droplet concentration to the PDPA-derived number concentration calculated in three different ways for six distributions with MVDs less than 18 μm, where no drizzle or precipitation-sized drops are present. The solid circles use the Anderson et al. (1993) collection efficiency curve and the PDPA channel midpoints to calculate the number of droplets expected to be collected by the CVI. While half the points are near the 1:1 line, the rest have PDPA number concentrations substantially larger than the measured CVI number concentrations. Based on the shape of the size distribution for the small MVD shown in Fig. A3 (appendix), we can assume that more droplets within a given size channel near the CVI cut size are smaller rather than larger than the midpoint; for example, in the 8–10-μm size channel, more drops are likely to be smaller than 9.0 μm rather than larger than 9.0 μm. This effectively biases the comparison when the CVI efficiency for 9.0 μm is assumed to represent the efficiency for all droplets in the 8–10-μm size range, since actual CVI collection efficiency is expected to vary substantially in this range. The hollow circles partially correct for this effect by using the CVI efficiencies based on the PDPA channel midpoint minus 0.5 μm. The hollow squares simply assume zero collection for droplets below 10.0 μm and 100% collection above 10.0 μm. As shown in the figure, the latter simplification gives results almost identical to those acquired using the Anderson et al. (1993) curve with a 0.5-μm correction, and both methods reproduce the actual measured CVI number concentration better than the midpoint approach. Ratios between number concentrations calculated from the PDPA using the simplified approach and the CVI number concentration range from 0.81 to 1.47, with a mean of 1.13.

Based on these results, CVI number concentrations, N_{CVI10}, were compared to PDPA number concentrations between 10- and 50-μm diameter, N_{PDPA10}, for the full range of study MVDs at 67 m s^{-1}. Figure 7 shows the CVI and PDPA number concentrations, and the ratio between the two, as a function of tunnel MVD. Much of the scatter between number concentrations (squares) for different runs at the same MVD is due to changes in tunnel liquid water content, which necessarily change the droplet number concentration for the same MVD. The solid symbols show the ratios of CVI to PDPA ($>$10 μm) number concentrations, which vary from near 1 at small MVDs up to 27 at the largest MVD, where substantial breakup of drops occurs.

The probability of drop breakup is determined by the Weber number, We, which is the ratio of destabilizing hydrodynamic force to stabilizing surface tension force. Drops will fragment when a critical value of the Weber number, We_c, is exceeded, and the type of breakup (e.g., bag, stripping, etc.) will change with We for $\mathrm{We} > \mathrm{We}_c$ (Pilch and Erdman 1987). Experimental data indicates that We_c for water drops is approximately 12 (Pilch and

TABLE 1. Regression results (r values) for N_{CV10}/N_{PDPA10} vs the bulk characteristics of the PDPA, 2D-C, and 2D-P at 67 m s^{-1}. CMP refers to composite values for combined PDPA, 2DC, and 2DP distributions; LWC is liquid water content, MVD is median volume diameter, and N is number concentration. Size ranges for 2DC and 2DP values included in the regression were 12.5 to 812.5 μm and 100 to 6500 μm, respectively, and r values $\geq$ 0.75 are boldface.

Parameter	Linear	Logarithmic	Sign
CMPLWC	0.34	0.56	+
CMP N	0.46	0.66	−
CMP MVD	**0.95**	**0.90**	+
PDPA LWC	0.41	0.18	−
PDPA N	0.46	0.66	−
PDPA MVD	0.70	**0.93**	+
2DC LWC	**0.78**	**0.90**	+
2DC N	0.16	0.53	+
2DC MVD	**0.84**	**0.95**	+
2DP LWC	**0.97**	**0.89**	+
2DP N	**0.93**	**0.89**	+
2DP MVD	0.21	0.08	−

Erdman 1987), although Tarnogrodzki (1993) developed a theoretical treatment that predicts values closer to 10 for water drops of the sizes considered here. Assuming $We_c = 12$, the critical diameter, d_c, or diameter of droplet expected to break up upon impaction in the CVI counterflow airstream, can be estimated:

$$We_c = \rho V_r^2 d_c/\sigma_w = 12, \quad (1)$$

$$d_c = 12\sigma_w/\rho V_r^2, \quad (2)$$

where ρ is the density of the medium (air), V_r is the relative velocity of air past the drop, and σ_w is the surface tension of water. For our conditions (temperature of 323 K and pressure of 987 mb), the critical diameter is about 169 μm at 67 m s^{-1} and 76 μm at 100 m s^{-1}. Schwarzenböck and Heintzenberg (2000) observed drop breakup using a ground-based CVI and obtained similar values at 100 m s^{-1} using theoretical considerations.

A drop that exceeds the critical We is expected to produce multiple fragments, with the number of fragments increasing with the initial drop size (Komabayasi et al. 1964). In most clouds, however, the concentration of large drops is many orders of magnitude lower than the total drop number concentration, which is dominated by the number of small droplets. As a result, drops near the critical We that break up and produce only a few fragments may not appreciably affect CVI number concentration. Drops with $We \gg We_c$, however, may produce many more drop fragments and significantly increase CVI number concentration. The ratio of CVI number concentration, N_{CVI10}, to PDPA number concentration larger than 10, N_{PDPA10}, was regressed against various other characteristics of the drop distributions in order to determine the variables most related to drop breakup. Characteristics included were MVD, LWC, and N for the PDPA alone (2–120 μm), the 2D-C alone (12–812 μm), and the 2D-P alone (100–6500 μm), as well as the composite values for all three probes. Results are shown in Table 1, with r values $\geq$ 0.75 in bold.

TABLE 2. Regression results (r values) for N_{CV10}/N_{PDPA10} vs characteristics of drops in various size ranges at 67 m s^{-1}. Boldface indicates r values $\geq$ 0.75.

Parameter	Linear	Logarithmic	Sign
62–162 μm N	0.42	**0.75**	+
162–312 μm N	**0.80**	**0.82**	+
312–700 μm N	**0.96**	**0.85**	+
>700 μm N	0.35	0.58	+
62–162 μm LWC	0.08	0.10	+
162–312 μm LWC	0.46	0.60	+
312–700 μm LWC	**0.96**	**0.88**	+
>700 μm LWC	0.41	0.39	+

Breakup is most obviously related to the overall MVD, the 2D-C LWC, the 2D-C MVD, the 2D-P LWC, and the 2D-P N. This clearly indicates that large drops contribute to drop breakup, and that both the number and size (which determine LWC) of large drops influence CVI number concentration. The PDPA MVD also is related to enhanced CVI number concentrations; however, this is most likely because distributions having larger MVDs in the small droplet size range also have more drops in the 2D-C and 2D-P range, as these parameters are not independent.

The previous analysis includes only bulk characteristics of a wide range of drop sizes. Based on the calculations given above, we would expect only drops larger than about 169 μm to break up at 67 m s^{-1}; even larger drops might be required to produce enough fragments to visibly affect CVI number concentration. Table 2 shows regression results based on drop number and liquid water content in four different size ranges: 62–162, 162–312, 312–700, and >700 μm (162 μm being the lower end of the 2D-C size bin that includes 169 μm drops). The strongest relationships are evident for drop number and liquid water content in the 312–700-μm range. Weaker, but significant, relationships exist with drop number and liquid water content in the 162–312 μm range. (Part of this correlation may be due to the strong relationship between the drop number in the 162–312-μm range and that in the 312–700-μm range; linear $r = 0.89$.) This indicates that drops larger than 312 μm have the largest influence on enhanced CVI number concentration, while drops between 162 and 312 μm play a smaller role. Drops larger than 700 μm are not strongly correlated with enhanced CVI concentrations, probably because they were present in such low number concentrations that they were not consistently collected by the CVI.

It would be useful under actual field conditions to have an indicator for when drop breakup is affecting CVI number concentration, in order to flag questionable data. The 2D-P LWC is strongly correlated with CVI-enhanced number concentration and is also a standard and simple parameter calculated from the 2D-P probe. Consequently, it is a suitable indicator. The magnitude

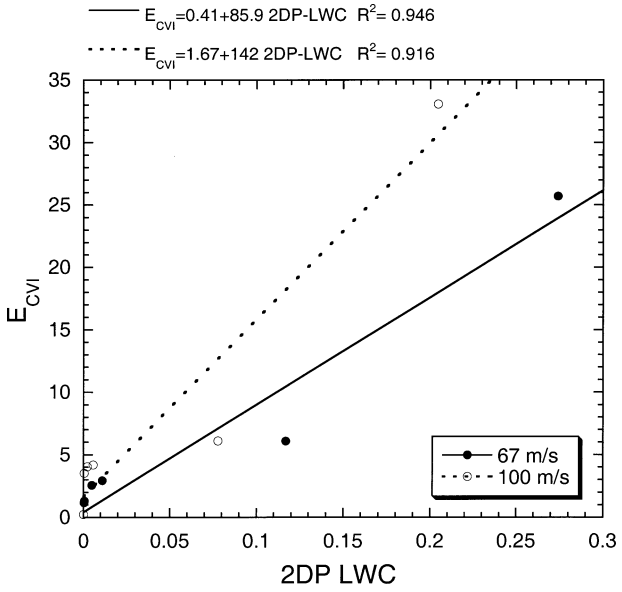

FIG. 8. CVI enhancement (ratio of CVI to PDPA number concentration shown later in Fig. A2 minus 1) as a function of 2D-P liquid water content in g m^{-3} at 67 m s^{-1} and at 100 m s^{-1}, where E_{CVI} values of zero indicate no enhancement. Due to the difference in cut sizes at 67 and 100 m s^{-1}, a PDPA number larger than 10 μm was used at 67 m s^{-1}, and a PDPA number larger than 8 μm was used at 100 m s^{-1}. The 2D-P was not used for many of the small-MVD runs. However, the 2D-P LWC was assumed to be zero if the 2D-C was available and it measured no liquid water (this assumption had to be used only once).

of enhancement in CVI number concentration, E_{CVI}, can be approximated as

$$E_{CVI} = (N_{CVIn}/N_{PDPAn}) - 1,$$

where n is the appropriate size cut for the measurement conditions. An E_{CVI} of zero indicates no enhancement. In Fig. 8, this value is plotted against the 2D-P liquid water content for 67 m s^{-1} with $n = 10$ and for 100 m s^{-1} with $n = 8$ (calculated cut size of 8.2 μm). While data points are sparse, E_{CVI} increases and is strongly correlated with 2D-P LWC at both airspeeds. The data indicate that significant enhancements can occur at quite low 2D-P water contents of less than 0.01 g m^{-3}. About twice as much enhancement occurs at 100 m s^{-1} as at 67 m s^{-1}, which might be expected due to the V_r^2 term in the Weber number. Also, the offset is higher at 100 m s^{-1}, suggesting that drops below the 2D-P size threshold (100 μm) may contribute to enhancement at 100 m s^{-1}. At 67 m s^{-1}, up to 0.000 22 g m^{-3} was measured without any significant enhancement in CVI number concentration, but enhancements of greater than 100% occurred at 2D-P LWCs of 0.000 57 g m^{-3}. At 100 m s^{-1}, 2D-P LWCs of 0.000 39 g m^{-3} led to enhancements of over 300%.

The addition of the inlet shroud for some runs as discussed in section 3b did not produce a consistent change in the ratio shown in Fig. 7. This indicates that breakup of drops on the shroud does not appreciably affect number concentrations within the CVI. Small drops produced by breakup on the shroud, with a relatively large internal diameter of 38 mm, most likely follow the streamlines around the much smaller CVI inlet tip.

4. Summary and conclusions

The NASA Icing Research Tunnel provides a valuable venue for testing instrument response to a range of droplet distributions and conditions. For droplet distributions with median volume diameters $\geq$ about 30 μm, liquid water content measured by the CVI agreed with reference values within the uncertainty of the measurements. For a range of LWCs at 30-μm MVD, the relationship was near 1:1, and no systematic dependence of CVI results on LWC or airspeed was observed. Thus, the CVI measures LWC with good accuracy in clouds with most of the water in mid- to large-sized drops. However, a significant discrepancy was observed between the amount of LWC measured by the CVI at small MVDs and that predicted based on the CVI collection efficiency measured during previous calibrations. A corresponding discrepancy was not observed in the comparison between drop number concentration measured by the CVI and the tunnel instruments, or in comparisons with in situ data. It is not yet known whether this discrepancy is due to uncertainty in the CVI collection efficiency under the tested conditions, to errors in the parameters determined by the tunnel instruments, or to a combination of both factors. Since the estimated uncertainties in each of these factors is lower than the differences observed, this discrepancy remains unexplained and warrants further investigation.

A few tunnel runs were repeated with a flow-straightening shroud around the CVI inlet. The shroud was designed to be isokinetic at higher (transonic) airspeeds but is predicted to be superisokinetic by about 20% at lower airspeeds. Corresponding increases in CVI LWCs of about 20% were observed for small droplet runs, as expected from modeling results.

The effect of large drop breakup on CVI number concentration was evaluated both theoretically and by comparing CVI number concentrations to concentrations in corresponding size ranges from the PDPA. Drop breakup was predicted to occur for drops larger than 169 μm at 67 m s^{-1} and larger than 76 μm at 100 m s^{-1}. Enhancement in number concentration at 67 m s^{-1} was found to be strongly related to large drop concentrations, with the number and liquid water content of drops in the 312–700-μm-diameter range being the most important parameters. Since drops in this size range dominated the LWC in the 2D-P range, the 2D-P LWC can be used as an indicator that drop breakup is likely to occur. Relatively large enhancements in CVI number concentration of a few hundred percent can occur even at 2D-P LWCs less than 0.01 g m^{-3}, increasing up to a factor of about 30 at 2D-P LWCs in the 0.20–0.30 g m^{-3} range.

About twice the amount of enhancement was observed at 100 m s^{-1} relative to 67 m s^{-1}. The shroud was found to have no appreciable affect on drop breakup.

Acknowledgments. We wish to acknowledge the donation of wind tunnel time by NASA and the professional assistance of Jack Oldenburg, Bob Ide, and the staff of the NASA IRT. The Federal Aviation Administration, Transport Canada, and the Meteorological Service of Canada (MSC) provided support for travel, and the Research Aviation Facility of NCAR supported the data analysis. Thanks also are due to the Centro Italiano Ricerche Aerospaziali for providing PDPA data, to Zlatko Vukovic of MSC for analysis of the 2D and PDPA data, and to Dave McFarland and Errol Korn at NCAR for technical support.

APPENDIX

CVI Sampling Efficiency at Small MVDs

In section 3a it was shown that the CVI undermeasured LWC in the wind tunnel at MVDs less than about 30 μm. These results are discussed with regard to current knowledge of the CVI collection efficiency and experimental data in real clouds in the atmosphere.

Collection efficiency has been measured in a number of calibration studies of ground-based CVIs, where a small wind tunnel is used to accelerate the air around the CVI probe. With the small wind tunnel design (in contrast to airborne probes), a reference cloud of mechanically generated droplets or particles can be introduced directly into the wind tunnel and accelerated up to the CVI inlet. Noone et al. (1988) impacted droplets of a known solute concentration, measured their dry size and concentration, and thereby inferred their equivalent wet droplet size and concentration as collected by the CVI. Anderson et al. (1993) and Schwarzenböck and Heintzenberg (2000) calibrated using glass beads of known sizes directly measured with an aerodynamic particle sizer. All these studies showed general agreement, particularly for the 50% cut size, with predictions of droplet stopping distance from aerodynamic drag theory.

The relatively sharp tip shape of the airborne CVI tested in the NASA Icing Research Tunnel is very similar to that of the ground-based CVI calibrated by Anderson et al. (1993). Thus, it has been assumed that those calibration results also can be applied to the airborne CVI, using the appropriate probe dimensions. One difference is that Anderson et al. (1993) used a much shorter porous tube inside the CVI; this was hypothesized to be one reason the Anderson et al. efficiency curve was sharper than that measured by Noone et al. (1988), who used a longer porous tube. The NCAR CVI also uses a longer porous tube. However, Fig. 4 shows that the Anderson et al. and Noone et al. curves give very similar results for the droplet distributions measured in the IRT, and therefore this is unlikely to be the source of the discrepancy in LWC at low MVDs.

Comparisons of CVI number concentration and LWC with FSSP-100 data in stratus clouds were reported by Twohy (1992), using cut sizes calculated from theory and assuming sharp efficiency curves. These comparisons showed good agreement between the CVI and FSSP results for liquid water content but relatively low efficiency for number concentration, which is determined from the number of residual droplet nuclei measured after evaporation downstream of the CVI inlet tip. The low number concentrations were hypothesized to be due to losses of residual droplet nuclei after impaction with internal inlet surfaces. Both wall losses of droplets due to off-axial trajectories and impaction of droplets with the 90° bend downstream of the inlet could produce this effect. Subsequent modifications to the CVI inlet were made to minimize these effects. These included the addition of a flow-straightening shroud upstream of the inlet, as well as a gradual increase to a larger internal diameter at the bend downstream of the inlet. As a result, CVI collection efficiency has been observed to increase.

For example, recent data collected in small trade wind cumuli on 11 March 1999 is shown in Fig. A1. Droplet concentration measured by the CVI (top trace) is compared with that expected to be collected by the CVI using the FSSP-100 size distribution and Anderson et al.'s (1993) calibration (middle trace). Number concentration is presented here, rather than LWC, because LWC derived from the FSSP size distribution has large uncertainty (e.g., Baumgardner et al. 1990). Laucks and Twohy (1998) employed a computational fluid dynamical model to predict the collection characteristics of an airborne CVI inlet. Their results, which were for a CVI inlet geometry that was similar to the one tested in the NASA tunnel, predicted substantially less-sharp impaction characteristics, with greatly reduced collection efficiencies above the cut size, than did those of Anderson et al. (1993). Expected droplet concentration calculated from the FSSP using the Laucks and Twohy (1998) efficiency curve is shown in the bottom trace. Measured CVI concentrations are generally closer to those predicted from the Anderson et al. (1993) empirical study, as detailed in Fig. A2.

Figure A2 shows regression results for 100-s averages of CVI and FSSP data taken on the 11 March flight, excluding time periods such as between 34 100–34 200 s when drizzle was present. (Number concentrations are rather low, since the 100-s averages include cloud edges and clear air as well as higher droplet concentrations in the cloud interiors.) Also shown are predicted concentrations using the Laucks and Twohy (1998) model and the Anderson et al. (1993) efficiency curve with 1.5- and 5.5-μm increases in cut size. The 5.5-μm increase is approximately what would be required to explain the IRT results shown in Fig. 4. The CVI and FSSP data are highly correlated, with R^2 values between 0.91 and

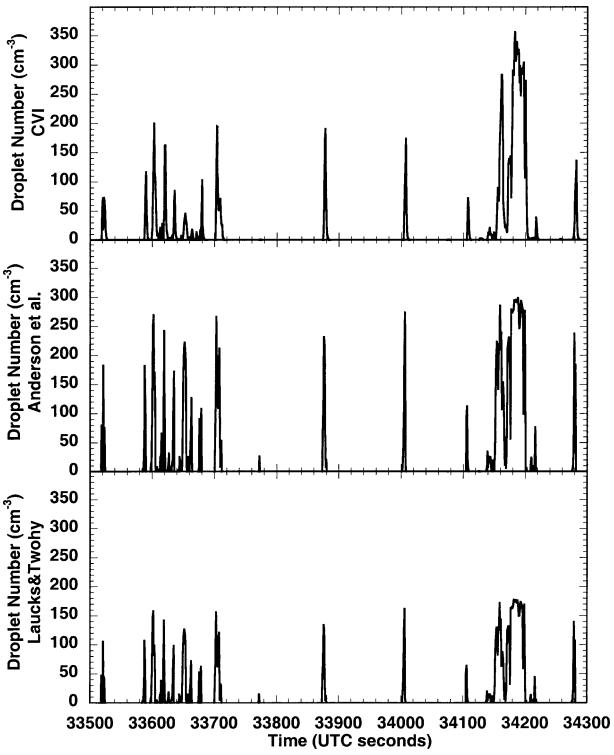

FIG. A1. Comparison of droplet number concentration measured by the CVI with that measured by the FSSP-100 on the NCAR C-130 aircraft in small tropical cumulus clouds on 11 Mar 1999. The top trace is residual droplet number measured by the CVI, the middle trace is droplet number concentration calculated from the measured FSSP-100 size distribution and the collection efficiency curve of Anderson et al. (1993), and the bottom trace is droplet number calculated from the FSSP-100 size distribution and the collection efficiency curve of Laucks and Twohy (1998). The CVI cut size was predicted to be 8.2 μm for these sampling conditions.

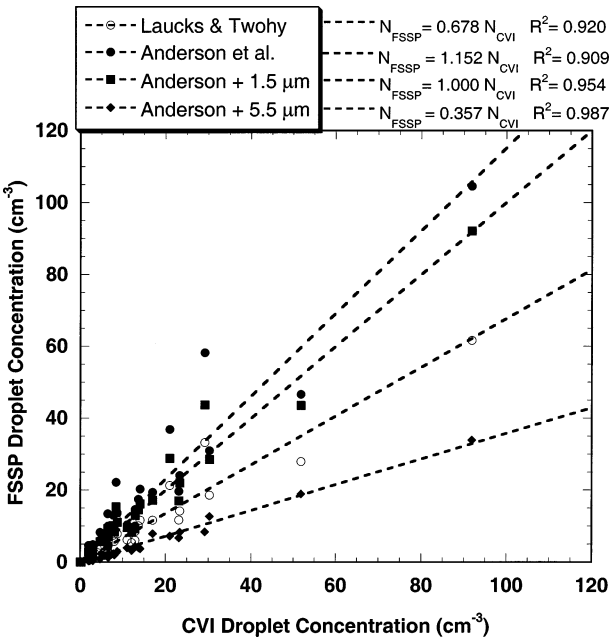

FIG. A2. CVI droplet number concentration from the 11 Mar 1999 C-130 flight vs that predicted from various collection efficiency curves and the measured FSSP-100 size distribution. Symbols represent 100-s averages of cloud and noncloud data.

0.99. Regression results show that the CVI concentrations are higher (by 47%, based on the inverse of the slope) than those predicted by the Laucks and Twohy (1998) model, and lower (by 13%) than those predicted from the Anderson et al. (1993) results. Increasing the Anderson et al. cut size by 1.5 μm leads to the best agreement, while increasing it to 5.5 μm produces large discrepancies.

These field results imply that the Anderson et al. (1993) results are generally applicable to the NCAR probe. While they suggest that the cut size of the NCAR probe may be slightly larger than predicted, the 13% difference between CVI measurements and the Anderson et al. predictions is within the uncertainty in the CVI and FSSP measurements. Also, settling and/or diffusional losses in the CVI probe and sampling lines may reduce CVI number concentration but should not affect LWC. Therefore, the large discrepancy between the expected and actual fraction of LWC measured in the IRT at small MVDs is not reproduced in this field study. Additionally, CVI measurements of LWC or ice water content in other studies (e.g., Twohy et al. 1997; Gerber et al. 1998) have agreed well with those from other probes measuring primarily smaller drops or crystals.

It may be important to note that high concentrations of small drops are always present in the IRT, even at large MVDs. This is a common property of most tunnel clouds due to the way in which droplets are generated by spray nozzles. Examples of a small-MVD and large-MVD size distributions are given in Fig. A3. The number concentration is dominated by drops smaller than

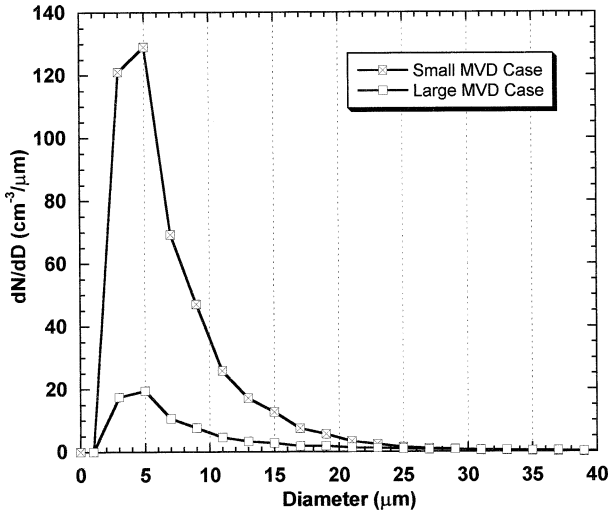

FIG. A3. Measured cloud number distributions in the wind tunnel at a small MVD (16.8 μm) and a large MVD (128.6 μm), showing that large concentrations of small droplets are always present.

10 μm, even in the large-MVD case, unlike what is typical for natural clouds. As a result, the mean diameter of all distributions tested in the tunnel is quite small, ranging from about 6.2 μm for a 12.9-μm MVD to just 12.3 μm for a 216-μm MVD; the mode diameter is even smaller.

Twohy (1998) showed that droplets smaller than the cut size may actually enter the slowly moving counterflow region inside the CVI tip before reversing direction and following the counterflow out the probe tip. One possibility is that these high concentrations of small droplets interact with larger droplets (e.g., by collision) in a way that shifts the CVI collection curve. Also, the size distribution is very steep in the region near the CVI cut size for small MVDs. This might contribute to larger errors in the calculated bulk properties of the distribution, which are based on the 2-μm-resolution channel midpoints used for the PDPA data. Finally, while the PDPA sizing is thought to be highly accurate, large corrections to its sample volume were required to produce accurate LWCs (Strapp et al. 2003).

Until the issues introduced here are better understood, the source of the discrepancy between CVI and tunnel values at small MVDs cannot be determined, and further study is needed.

REFERENCES

Anderson, T. L., and C. H. Twohy, 1993: Collection and exclusion of large cloud elements with a counterflow virtual impactor. Abstracts, *AAAR 12th Annual Conf.*, Oak Brook, IL, American Association for Aerosol Research, 36.

——, R. J. Charlson, and D. S. Covert, 1993: Calibration of a counterflow virtual impactor at aerodynamic diameters from 1 to 15 μm. *Aer. Sci. Technol.,* **19,** 317–329.

Baumgardner, D., W. A. Cooper, and J. E. Dye, 1990: Optical and electronic limitations of the forward-scattering spectrometer probe. *Liquid Particle Size Techniques,* E. D. Hirleman, W. D. Bachalo, and P. G. Felton, Eds., Vol. 2, ASTM Standard Tech. Publication 1083, American Society for Testing and Materials, 115–127.

Coleman, H. W., and W. G. Steele, 1999: *Experimentation and Uncertainty Analysis for Engineers.* John Wiley and Sons, 2d ed. 275 pp.

Gerber, H., C. H. Twohy, B. Gandrud, A. J. Heymsfield, G. M. McFarquhar, P. J. DeMott, and D. C. Rogers, 1998: Measurements of wave-cloud microphysical properties with two new aircraft probes. *Geophys. Res. Lett.,* **25,** 1117–1120.

Komabayasi, M., T. Gonda, and K. Isono, 1964: Life time of water drops before breaking and size distribution of fragment drops. *J. Meteor. Soc. Japan,* **42,** 330–340.

Laucks, M. L., and C. H. Twohy, 1998: Size-dependent sampling efficiency of an airborne counterflow virtual impactor. *Aer. Sci. Technol.,* **28,** 40–61.

Noone, K. J., J. A. Ogren, J. Heintzenberg, R. J. Charlson, and D. S. Covert, 1988: Design and calibration of a counterflow virtual impactor for sampling of atmospheric fog and cloud droplets. *Aer. Sci. Technol.,* **8,** 235–244.

Ogren, J. A., J. Heintzenberg, and R. J. Charlson, 1985: In-situ sampling of clouds with a droplet to aerosol converter. *Geophys. Res. Lett.,* **12,** 121–124.

Pilch, M., and C. A. Erdman, 1987: Use of breakup time data and velocity history data to predict the maximum size of stable fragments for acceleration-induced breakup of a liquid drop. *Int. J. Multiphase Flow,* **13,** 741–757.

Schwarzenböck, A., and J. Heintzenberg, 2000: Cut size minimization and cloud element break-up in a ground-based CVI. *J. Aerosol Sci.,* **31,** 477–489.

Strapp, J. W., and Coauthors, 2003: Wind tunnel measurements of the response of hot wire liquid water content instruments to large droplets. *J. Atmos. Oceanic Technol.,* **20,** 791–806.

Ström, J., and J. Heintzenberg, 1994: Water vapor, condensed water, and crystal concentration in orographically influenced cirrus clouds. *J. Atmos. Sci.,* **51,** 2368–2383.

Tarnogrodzki, A., 1993: Theoretical prediction of the critical Weber number. *Int. J. Multiphase Flow,* **19,** 329–336.

Twohy, C. H., 1992: On the size dependence of the chemical properties of cloud droplets: Exploratory studies by aircraft. NCAR Cooperative Thesis CT-137, Ph.D. dissertation, University of Washington and National Center for Atmospheric Research, 239 pp.

——, 1998: Model calculations and wind tunnel testing of an isokinetic shroud for high-speed sampling. *Aer. Sci. Technol.,* **28,** 261–280.

——, A. J. Schanot, and W. A. Cooper, 1997: Measurement of condensed water content in liquid and ice clouds using an airborne counterflow virtual impactor. *J. Atmos. Oceanic Technol.,* **14,** 197–202.

Wendisch, M., T. J. Garrett, and J. W. Strapp, 2002: Wind tunnel tests of airborne PVM-100A response to large droplets. *J. Atmos. Oceanic Technol.,* **19,** 1577–1584.